The Fifth International Symposium on Computational Wind Engineering (CWE2010)
Chapel Hill, North Carolina, USA May 23-27, 2010

Prediction of street canyon velocities

Terianne Hall[a], Rex Britter[b], Leslie Norford[c]

[a]*Massachusetts Institute of Technology, Cambridge, MA, USA, teri85@mit.edu*
[b]*Massachusetts Institute of Technology, Cambridge, MA, USA, rexb@mit.edu*
[c]*Massachusetts Institute of Technology, Cambridge, MA, USA, lnorford@mit.edu*

ABSTRACT: We created an empirical model using analytical formulas to predict the bulk velocities in street canyons and the shear stress on rough urban surfaces based on atmospheric velocity, average size and distribution of obstructions characteristic of building surfaces, and canyon orientation. The model is based on control volume arguments, entrainment and exchange processes, connections between the Nikuradse sand grain roughness and both the skin friction coefficient and the form of complex urban surfaces, and correlations for the urban canyon problem found using CFD in a generic form. This work can be applied at a neighborhood scale both analytically, using spatially averaged neighborhood parameters, and in simulation, using a shear stress boundary condition to approximate rough urban surfaces.

1 MOTIVATION AND BACKGROUND

This purpose of this work is to better understand and predict how air moves through a city and how it carries pollutants, sensible and latent heat, and toxic chemicals arising from accidental releases. Where will the plume of released pollutant go and how can we mitigate the urban heat island effect by changing the form of the city?

Pollutants, such as vehicle emissions, released into the heavily populated urban canopy layer are retained there unless removed into the urban boundary layer (Oke, 1987). Insufficient removal of pollutants is a result of weak turbulent exchange between the urban canopy layer and the urban boundary layer, and this can be directly attributed to building geometry, the urban form and meteorology (Britter and Hanna, 2003). The ability to predict areas that are prone to high pollutant concentrations allows urban planners and architects to make informed decisions about matters such as the placement of sidewalks and building air intakes.

Poorly planned urban development can lead to significantly higher temperatures in the urban canopy layer, particularly at night, which in many climates results in decreased thermal comfort for pedestrians and residents and increased building energy consumption. Because man-made materials have different thermal properties and geometries than natural materials, the microclimate of the urban area is different than that of neighboring rural areas. With urbanization, the heat storage capacity of the city is increased due to increased surface area (from buildings) that is available to absorb and reflect short wave radiation. Buildings and streets in a street canyon absorb short wave radiation all day, and would normally reradiate it via long wave radiation to the cooler night sky, however building geometry decreases the surface view factor associated with radiative cooling (Oke, 1987). Building geometry further contributes to the UHI phenomenon by decreasing the wind speed, and, consequently the advective cooling of building surfaces. Another cause of the UHI is increased waste heat contributed to the urban microclimate by anthropogenic activities and industry. This includes waste heat expelled by automobiles and by building air conditioning units – which is particularly relevant in many tropical cities that have a "cooling" climate throughout the year. Like pollutants, predicting how sensible and latent heat travels and

is stored in the city, both spatially and temporally, will result in informed decision making by urban planners.

2 STREET CANYON PARALLEL TO THE ATMOSPHERIC FLOW

Idealized cities are often considered as a series of blocks that act as roughness elements to the atmospheric flow above (Cheng and Castro, 2002). Using this approach, we simulated the airflow around a grid of evenly spaced cubic buildings with a logarithmic wind profile at the inlet. The aspect ratio of the canyons was approximately unity (Figures 1a and 1b). As the flow approached the bluff buildings and entered the canyons there was a contraction effect at the first row of buildings – initially there was an increase in the longitudinal bulk velocity along the canyon. After the contraction, the longitudinal bulk velocity decreased rapidly in the canyons between the next rows of buildings – the decrease in velocity was due to a reduction in momentum induced by a drag force on the flow from the building façades. Air was expelled from the street canyon to the atmosphere along this part of the canyon by mass continuity. The remaining rows of buildings exhibited little change in longitudinal bulk velocity – in this section of the canyon, the flow was fully developed. This is in agreement with Dobre et al (2005); they make observations about the flow in a real intersection in London based on the idealization of an infinitely long street with the assumption that there is no vertical motion associated with the longitudinal canyon flow.

Assuming fully developed flow allows us to consider the simplest idealization of a neighborhood: a plane with a series of notched channels (Skote et al, 2005). The urban boundary layer flow can be approximated as fully developed flow over a rough plate. This raises the question: what drives the flow in the urban canopy layer, specifically, what overcomes the decrease in momentum from the shear stress on the fluid imposed by the canyon walls? If the street canyons were four-sided ducts the flow would be pressure driven, but is there a pressure drop along the canyon? What about along the entire neighborhood? We addressed these questions using Fluent 6.3 by studying three cases with typical canyon geometry: a four-sided duct, a three-sided channel enclosed by a fourth wall with a slip boundary condition, and a three-sided channel with an expansive volume enclosed by slip boundary conditions above, as depicted in Figure 1a. All of the cases were run with a fixed mass flow rate and periodic boundary conditions on the inlet and outlet to allow the flow to become fully developed. The first two cases behaved as expected – the flow was pressure driven, and the magnitudes of the pressure drops were consistent with pipe theory. The pressure drop was very small in the case with the expansive volume. The air above the canyon was driven by the negligible pressure drop, and momentum exchange with this large air mass drove the flow in the canyon. This scenario can be studied analytically with control volume arguments.

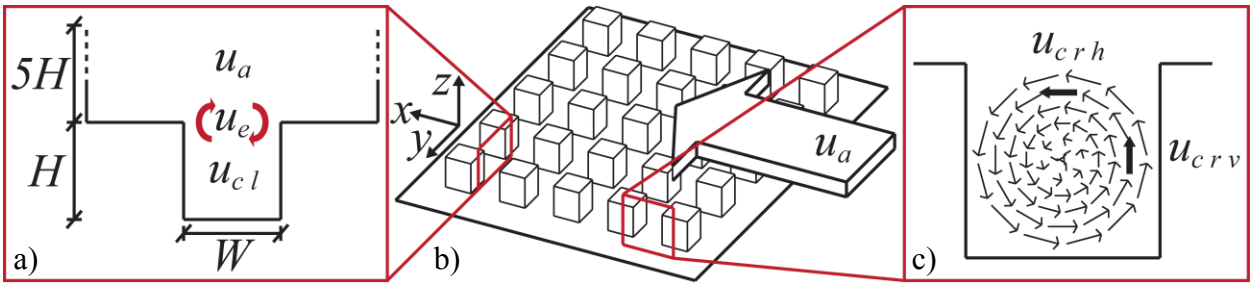

Figure 1: a) cross sectional view of canyon that parallel to atmospheric flow, idealized as three-sided duct with expansive volume above; b) grid of evenly spaced buildings; c) cross sectional view of canyon that is perpendicular to atmospheric flow

Recall the equation for linear momentum for a control volume:

$$\sum \vec{F}_{CV} = \frac{d}{dt}\int_{CV} \rho u \, dV + \oint_{CS} \rho u (\vec{v} \cdot \vec{n}) \, dA \tag{1}$$

where F_{CV} is any force on the control volume, ρ is the density of the fluid, u and v are velocities, V is the volume of the control volume, and A is the area of the control surfaces. Consider a control volume enclosing the urban canopy layer in a street canyon parallel to the atmospheric wind. For the fully developed and steady state case where the shear stress applied to the fluid by the building façades and the ground must be balanced by a momentum flux across the top surface of the canyon, Equation 1 can be rewritten as

$$-\int_{CS-ground} \tau \, dA - \int_{CS-left\,wall} \tau \, dA - \int_{CS-rightwall} \tau \, dA = \int_{CS-top} \rho u_e \, u_{cl} \, dA - \int_{CS-top} \rho u_e \, u_a \, dA \tag{2}$$

where τ is the shear stress applied to the fluid by building façades and ground, u_a is the characteristic atmospheric velocity, u_{cl} is the spatially averaged longitudinal bulk velocity in the canyon, and u_e is the spatially averaged exchange velocity between the street canyon and the atmospheric flow as defined by Bentham and Britter (2003). The exchange velocity is in the vertical direction and the net vertical velocity in the fully developed flow case is zero, to conserve mass. The shear stress on the walls surrounding the canyon is given by

$$\tau = \rho u_*^{\,2} = \frac{C_f \, \rho u_{cl}^{\,2}}{2} \tag{3}$$

where u_* is the friction velocity for the canyon floor and walls and C_f is the skin friction coefficient of these surfaces. For the control volume enclosing a canyon parallel to the atmospheric flow, Equations 2 and 3 can be rearranged and simplified to find an expression for the ratio between the canyon velocity and the atmospheric velocity, and this is a useful parameter when considering early stage urban design.

$$\left(\frac{u_{cl}}{u_a}\right) = \left(\sqrt{\frac{C_f \left(\frac{H}{W} + \frac{1}{2}\right)}{\alpha}} + 1 \right)^{-1} \tag{4}$$

where H is the height of the canyon, W is the width of the canyon, and α is an exchange coefficient inspired by the plume entrainment theory of Morton et al (1956). We define the exchange coefficient for flow along the canyon as

$$\alpha = \frac{u_e}{u_a - u_{cl}}. \tag{5}$$

In the case of a street canyon that is parallel to the flow, u_{cl} and u_a are in the same direction. The relative velocity in the denominator of Equation 5 is representative of the shear near the top of the canyon. This generates a shear stress in the fluid and turbulent mixing between the urban canopy layer and the urban boundary layer above. The exchange coefficient is constant for a given geometry (Bentham and Britter, 2003). This means that knowing atmospheric wind velocity, geometry of the canyon, and the skin friction coefficient of the canyon surfaces, we can analytically determine a good approximation to the bulk longitudinal velocity in the canyon.

2.1 *What is the skin friction coefficient of a real street canyon?*

The skin friction coefficient,

$$C_f = \frac{2\tau}{\rho u_\infty{}^2}, \tag{6}$$

is a non-dimensional measure of the surface shear stress and is a function of the surface roughness, where u_∞ is the characteristic free stream velocity of the fluid flowing over the surface. Real street canyons are often covered with balconies and air-conditioners units, and in densely populated areas the streets are filled with cars and buses. This surface roughness will lead to increased shear stress on the surfaces and decreased longitudinal velocities in the canyon. Additionally, these obstructions could lead to increased turbulence in the canyon flow, and could lead to an increase in the turbulent exchange between the above-canyon and in-canyon flows.

The skin friction coefficient can be translated to physical roughness elements using two empirical relationships. First, the skin friction coefficient can be directly related to the Nikuradse sand grain roughness by the Moody Diagram (Figure 2a). The purple box drawn on the Moody Diagram in Figure 2a depicts the region relevant to canyon flow. The range of Reynolds numbers is based on typical canyon geometry and wind speeds. The range of relative roughness is based on empirical relationships collected by Koloseus and Davidian (1966). They combined a wealth of experimental data to relate roughness element heights to the Nikuradse sand grain roughness for a variety of obstruction types (Koloseus and Davidian 1966). These relationships are displayed in Figure 2b.

Along canyon flow is in the fully rough regime, thus the relationship between the friction factor and the relative roughness is independent of Reynolds number. This empirical relationship is

$$f = 4C_f = \left(1.74 + 2\log_{10}\left(\frac{D_h}{2k_s}\right)\right)^{-2} \tag{7}$$

where f is the moody friction factor, k_s is the Nikuradse sand grain roughness, and D_h the hydraulic diameter (or some characteristic length) (Nikuradse, 1950). The hydraulic diameter of a street canyon can be approximated to that of a rectangular duct.

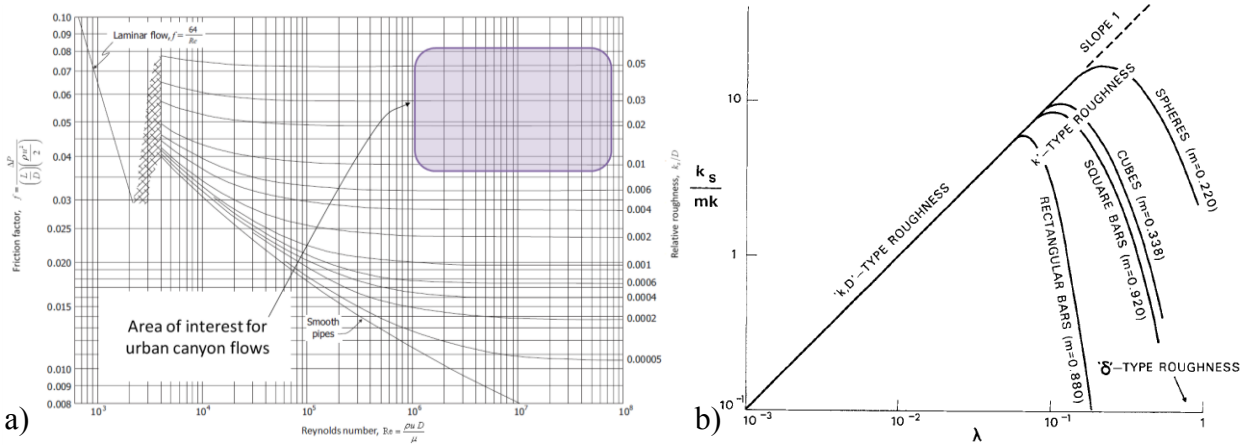

Figure 2: a) Moody diagram for pipe flow(adapted from Walski et al, 2003); b) Variation of equivalent roughness height with concentration of roughness elements, indicating the approximate ranges of various 'roughness regimes'. Here roughness concentration λ = (frontal area per element) / (specific area), k_s is the equivalent sand-grain roughness height of Nikuradse, and k is roughness height. The 'coalescing factor' m, has been adjusted empirically to give unit slope in the straight-line range of the data (Koloseus and Davidian 1966).

2.2 *Predicting longitudinal bulk velocity in a street canyon parallel to the flow*

Assuming flow around a rectangular cuboid-shaped balcony is almost the same as flow around a cube, the relationships displayed in Figure 2b define an equivalent sand grain roughness for a canyon wall, knowing only the frontal to plan area ratio associated with the roughness elements on the canyon surface. If we concede that many canyon roughness elements can be approximated as cubes, then we can use the empirical relationships displayed in Figures 2a and 2b to translate the roughness of a real building façade into an equivalent skin friction coefficient. We find the range for reasonable skin friction coefficients for street canyons is small: 0.007 to 0.02.

The appropriate range for the exchange coefficient in an urban setting is 0.01 to 0.10 (MacDonald et al, 1998; Bentham and Britter, 2003). Using these ranges we can produce graphical representations of Equation 4 (Figures 3a and 3b). In Figure 3a, the skin friction coefficient is held constant at 0.016, and in Figure 3b the aspect ratio of the street canyon is unity. The exact value of the exchange coefficient will be determined by the geometry of the neighborhood surrounding the canyon. Future work will compare these graphs with CFD and experimental results.

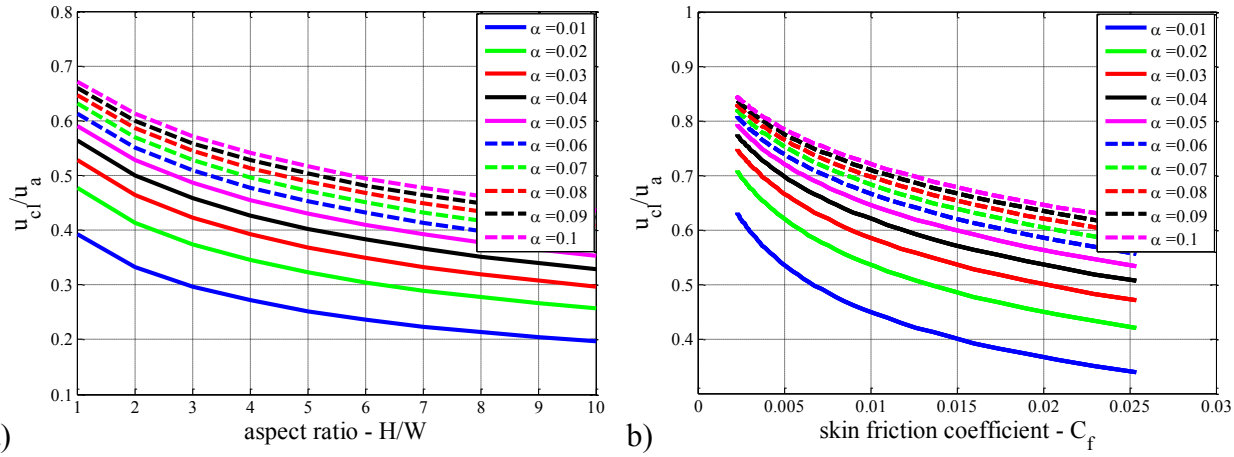

Figure 3: a) u_{cl}/u_a vs. aspect ratio for a canyon with a skin friction coefficient of 0.016; b) u_{cl}/u_a vs. skin friction coefficient for a canyon with an aspect ratio of unity

3 STREET CANYON PERPENDICULAR TO THE ATMOSPHERIC FLOW

The most commonly studied canyon flow is that where the atmospheric flow is perpendicular to the axis of the street canyon. These flows are characterized by one or more recirculating vortices in the canyon, and the number of vortices is generally dependent on the aspect ratio of the canyon (*H*/*W*) (Hosker, 1985; Britter and Hanna, 2003). Like the longitudinal case, the perpendicular case has an exchange velocity which is responsible for ventilating the canyon. We define an exchange coefficient for the recirculating case as

$$\alpha = \frac{u_e}{u_a - u_{crh}} \rightarrow \frac{u_e}{u_a} \tag{8}$$

where u_{crh} is defined here as the spatially averaged component of the rotational velocity that is horizontal (Figure 1c). This component of the canyon flow is perpendicular to both the longitudinal bulk velocity and the vertical velocity associated with the vortex. The exchange coefficient is constant for a given geometry, and in the case of a street canyon that is perpendicular to the flow, u_{crh} and u_a are in the same direction. In the ideal perpendicular case, both u_{crh} and u_{cl} are zero.

4 STREET CANYON AT AN ANGLE TO THE ATMOSPHERIC FLOW

When the canyon is at an angle to the atmospheric flow, the flow in the canyon is thought to be a combination of recirculating flow and longitudinal flow. This scenario is the most realistic, yet it is less studied than the cases where the wind is aligned with or perpendicular to the canyon (Soulhac et al, 2008). Dobre et al (2005) looks at experimental results from the DAPPLE project for a canyon at an angle to the atmospheric flow. They found that both the longitudinal and recirculating flow velocities varied linearly with the component of the atmospheric velocity along the parallel and perpendicular axes of the canyon respectively. This is in agreement with the relationship derived in Equation 4; the right hand side of the equation is a constant for a particular canyon. Soulhac et al (2008) compares an analytical model based on flow regime to numerical simulation for various wind directions and canyon aspect ratios. Their results agree with Dobre et al (2005) and Equation 4 for most canyon orientations. An unexpected result is their finding that for many canyon angles, the bulk longitudinal velocity in the canyon divided by the component of the atmospheric velocity that is parallel to the canyon is independent of canyon angle. Equation 4 can then be extended to canyons that are up to 60º from being parallel to the atmospheric flow.

Both Dobre et al (2005) and Soulhac et al (2008) worked in rotated coordinate systems; however for the purposes for the exchange coefficient we chose a coordinate system that is aligned with the atmospheric flow and x, y, and z are as in Figure 1. The angle between the canyon and the atmospheric flow, θ, is defined as a positive rotation from the x-direction about the vertical z-axis. Coordinate transformations are displayed for clarity below:

$$u_{cl} = u_{cx}\cos\theta + u_{cy}\sin\theta; \tag{9}$$

$$u_{crh} = u_{cx}\sin\theta - u_{cy}\cos\theta. \tag{10}$$

In these transformations, the rotational and longitudinal canyon velocities are defined such that the transformed velocity component is positive in the atmospheric direction.

The exchange of air between the urban boundary layer and the urban canopy layer varies with the relative velocity between the atmospheric flow and the flow in the canyon that is parallel to the atmospheric flow. We define the exchange coefficient in both coordinate systems as

$$\alpha = \frac{u_e}{u_a - (u_{cl}\cos\theta + u_{crh}\sin\theta)} = \frac{u_e}{u_a - u_{cx}}. \tag{11}$$

5 HOW DOES THE EXCHANGE VELOCITY VARY WITH CANYON ORIENTATION?

We simulated street canyons with various orientations to the wind to study the momentum exchange at the top surface of the canyon. The simulations were performed with Fluent 6.3 with a fixed mass flow rate and periodic boundary conditions on the inlet and outlet to ensure fully developed flow. The two building façades and the ground were modeled as smooth walls, and all other sides of the domain were given slip boundary conditions.

The points in Figure 4 show the variation of u_{cx}/u_a for the range of angles studied. In Soulhac et al (2008), they find that $u_{cl}/(u_a\cos\theta)$ = constant over a range of angles. Assuming this is true for the spatially averaged rotational velocity as well, that is $u_{crh}/(u_a\sin\theta)$ = constant, then these relationships can be combined with Equations 9 and 10 to find

$$\frac{u_{cx}}{u_a} = \beta \cos^2 \theta + \gamma \sin^2 \theta \tag{12}$$

where β and γ are the constants associated with longitudinal flow and rotational flow respectively. For an ideal canyon, γ is zero, and β is the right hand side of Equation 4. We chose β to fit our longitudinal simulated result, and plotted Equation 12 as the solid line in Figure 4. Because α should not vary with canyon orientation, we chose a value of 0.05 to visualize how u_e varies with θ. The result is normalized by the atmospheric velocity, and is shown as the dashed line in Figure 4. Both of these curves can be approximated as linear for the purposes of our simple model.

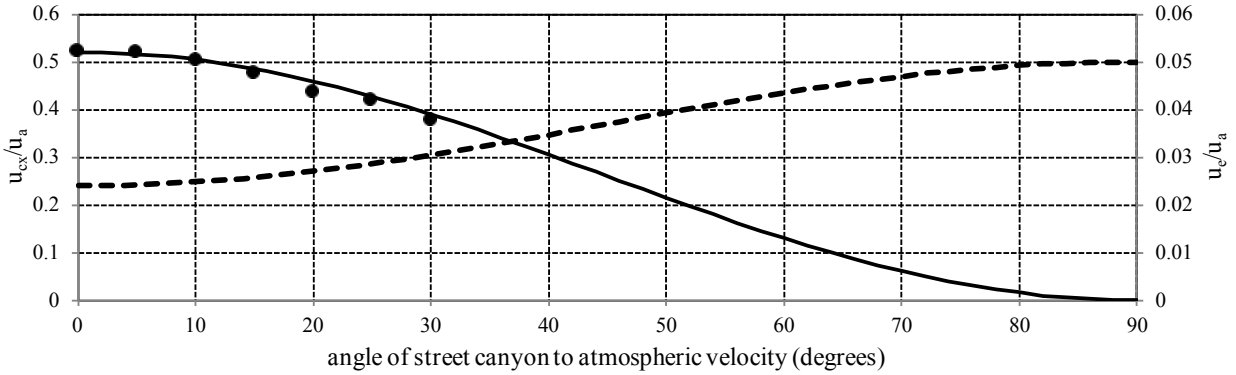

Figure 4: u_{cx}/u_a and u_e/u_a vs. angle of street canyon to atmospheric velocity for a canyon with an aspect ratio of unity

6 NEIGHBORHOOD SCALE APPLICATIONS AND FUTURE WORK

Results comparing our model to explicitly modeled surface roughness elements have been promising. Preliminary results for flow parallel to the canyon are displayed in Figure 5 for the idealized domain in Figure 1a with periodic boundary conditions on the inlet and the outlet of the domain, and slip boundary conditions on all non-canyon surfaces. The domain on the left side of Figure 5 has two smooth walls and one wall with 1x1x3m balconies spaced every 10m horizontally and 4m vertically. Approximating these balconies as cubes and using the relationships derived from Figure 2, the wall has an equivalent C_f of 0.016. This value was used in Equations 3 and 4 to predict the equivalent shear stress on the right building façade. The calculated shear stress was then used as a boundary condition on the right building façade. In the future, the shear stress boundary condition can be used in lieu of explicitly modeled balconies to decrease meshing time and runtime for neighborhood scale CFD models. At this point, the exchange coefficient can be tuned to longitudinal flow results, however further evaluation of the model is necessary.

We can relate our exchange coefficient to neighborhood geometry using the semi-empirical model developed by MacDonald et al (1998) and the analytical model developed by Bentham and Britter (2003) (Figure 6a). Here, λ_f is considered as a spatially averaged neighborhood parameter, though it is directly related to H/W. The data in Figure 6a implies that there is less turbulent exchange in sparsely developed neighborhoods. As the neighborhood becomes more built-up, turbulent exchange increases until the flow structure over the buildings becomes more like skimming flow, and then turbulent exchange decreases. Figure 6b suggests that as a neighborhood becomes more built-up, the average bulk longitudinal velocity in the urban canopy layer decreases. Linking our canyon model to neighborhood scale geometry will allow us to predict the turbulent exchange of a particular canyon based on its geometry, roughness and its surroundings. Populating Figures 3 and 6 with simulations and experimental measurements for various canyon geometries and neighborhoods will help us understand what is most important for predicting α.

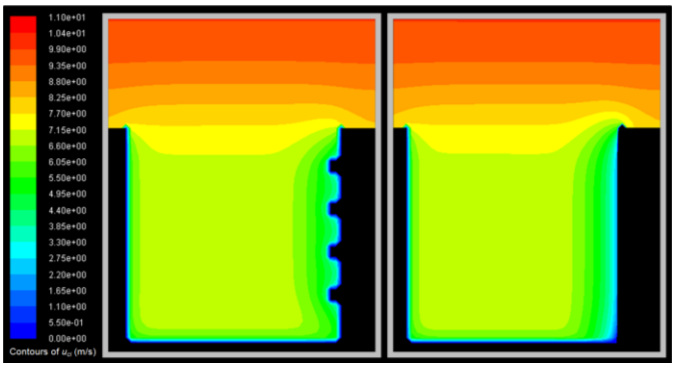

Figure 5: left – explicitly modeled roughness elements; right – shear stress boundary condition

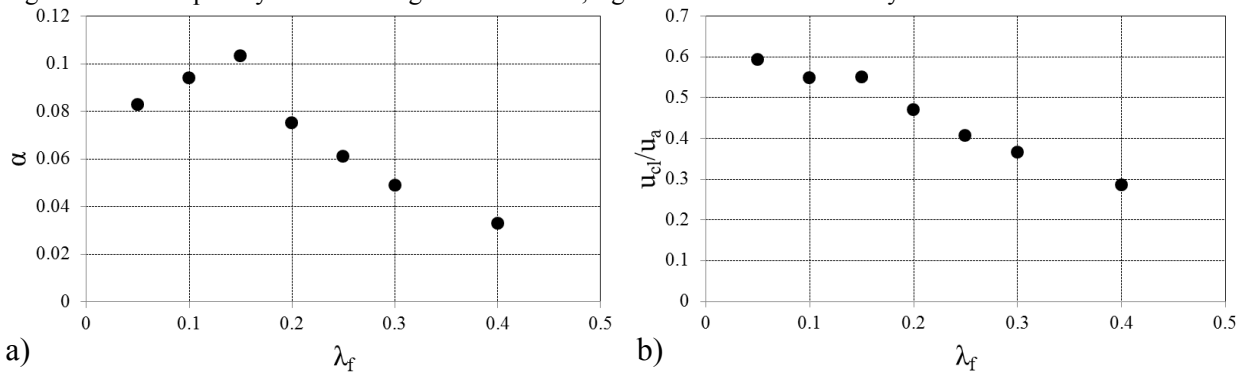

Figure 6: a) α vs. λ_f spatially averaged over a neighborhood, λ_f = (frontal area per element) / (specific area); b) u_{cl}/u_a vs. λ_f spatially averaged over a neighborhood; (based on MacDonald et al, 1998; Bentham and Britter, 2003)

7 ACKNOWLEDGEMENTS

The research described in this paper was funded by the Singapore National Research Foundation through the Singapore-MIT Alliance for Research and Technology Center for Environmental Sensing and Modeling. Britter acknowledges support from the Senseable City Laboratory, MIT.

8 REFERENCES

Bentham, J.T., Britter, R.E., 2003. Spatially averaged flow within obstacle arrays. Atmos. Environ. 37, 2037-2043.
Britter, R.E. and Hanna, S.R., 2003. Flow and dispersion in urban areas. Annual Rev. of Fluid Mech. 35, 469-496.
Cheng, H. and Castro, I.P., 2002. Near wall flow over urban-like roughness. Boundary-Layer Met. 104, 229-259.
Dobre, A. et al, 2005. Flow field measurements in the proximity of an urban intersection in London, UK. Atmos. Environ. 39, 4647–4657.
Hosker, R.P., 1985 Flow around isolated structures and building clusters: a review. ASHRAE Trans. 91, 1671–1692.
Koloseus, H.J., Davidian, J., 1966. Free surface instability correlations and roughness-concentration effects on flow over hydrodynamically-rough surfaces. USGS Water-Supply Paper 1592-C, D.
MacDonald, R.W. et al, 1998. An improved method for estimation of surface roughness of obstacle arrays. Atmos. Environ. 32, 1857–1864.
Morton, B.R. et al, 1956. Turbulent gravitational convection from maintained and instantaneous sources. Proceedings of the Royal Society of London. Series A, Mathematical and Physical Sciences 234(1196), 1-23.
Nikuradse, J., 1950. Laws of flow in rough pipes. NACA TM 1292. (Translation of VDI-Forchungsheft 361, 1933)
Oke, T.R., 1987. Boundary Layer Climates, 2nd edition, London.
Skote, M. et al, 2005. Numerical and experimental studies of wind environment in an urban morphology. Atmos. Environ. 39, 6147-6158.
Soulhac, L. et al, 2008. Flow in a street canyon for any external wind direction. Boundary-Layer Met. 126, 365-388.
Walski, T.M. et al, 2003. Advanced water distribution modeling and management. Haestad Press, Waterbury, CT.